JOURNAL OF Applied Polymer SCIENCE

Dielectric Strength of Al_2O_3/Silicone Composites After High-Temperature Aging

Yiying Yao,[1] Zheng Chen,[2] Guo-Quan Lu,[1,2] Dushan Boroyevich,[2] Khai D. T. Ngo[2]
[1]Department of Materials Science and Engineering, Center for Power Electronics Systems, Virginia Polytechnic Institute and State University, Blacksburg, Virginia 24061
[2]Department of Electrical and Computer Engineering, Center for Power Electronics Systems, Virginia Polytechnic Institute and State University, Blacksburg, Virginia 24061
Correspondence to: G.-Q. Lu (E-mail: gqlu@vt.edu)

ABSTRACT: Silicones are widely used for electrical insulation owing to their high dielectric strength and thermal stability. However, recent studies revealed insufficient stability of silicone for high-temperature applications. To study the effect of Al_2O_3 fiber on silicone stability, we measured the dielectric strength of unfilled silicone and Al_2O_3/silicone composites as a function of aging time at 250°C in air and analyzed data by Weibull probability distribution to determine characteristic dielectric strength (E_0) and shape parameter (β). Prior to aging, unfilled silicone and composites had similar behavior, with E_0 at about 20 kV/mm and $\beta > 15$. During aging, unfilled silicone developed both micro- and macrocracks, with β dropped below five in 240 h and E_0 decreased significantly. Composites developed microcracks, with β dropped below 5 in longer time and E_0 remained almost constant. Addition of Al_2O_3 slowed down crack growth in silicone matrix, resulting in longer lasting high-temperature dielectric materials. © 2014 Wiley Periodicals, Inc. J. Appl. Polym. Sci. **2014**, *131*, 41170.

KEYWORDS: ageing; composites; dielectric properties; elastomers; packaging

Received 13 April 2014; accepted 16 June 2014
DOI: 10.1002/app.41170

INTRODUCTION

Components on circuit boards or in electronic modules are usually covered with polymeric encapsulants to protect them against adverse environmental conditions (e.g., moisture, contaminants, mobile ions, radiations, and mechanical damages) and to increase their reliability.[1,2] In power electronics, a high dielectric strength of encapsulants (usually, ≥10 kV/mm) is required to prevent breakdown in the package.[3] Because of the development and commercialization of wide-bandgap devices, which can operate at a junction temperature of 250°C, the high dielectric strength of encapsulants needs to be maintained at or above 250°C to guarantee high-temperature operation.

Because of their high dielectric strength, excellent chemical resistance, and high thermal stability, silicones are widely used for encapsulating power electronic modules. Nowadays, high-temperature silicone-based encapsulants are claimed by their manufacturers to be capable of operating at temperature up to 300°C.[4–6] However, recent studies[7,8] on long-term reliability of silicone encapsulants suggested that commercial high-temperature silicones, when being aged at 250°C, could suffer from severe thermal degradation. Therefore, the thermal stability of commercial silicones must be improved to encapsulate wide-bandgap devices with high operation temperatures.

It has been widely reported in the literature that the thermal stability of silicones can be improved by adding fillers (such as SiO_2, Al_2O_3, and layered silicate[9–20]), which possibly interact with the polymer matrix and restrict chain mobility. A previous article of ours[21] reported that the results of weight-loss experiments indicated that thermal stability of silicone could be improved by adding Al_2O_3 fibers. In this study, the effect of Al_2O_3 fibers on thermal stability of silicone is investigated by monitoring the change in dielectric strength during thermal aging. Further aging can adversely affect dielectric strength when degradation is significant enough to weaken and crack the material. Therefore, change in dielectric strength is used as an indication of silicone degradation. The dielectric strength of unfilled silicone and Al_2O_3/silicone composites with various Al_2O_3–fiber loading is compared before and after thermal aging at 250°C in air. A more thermally stable material is expected to experience slower degradation and maintain its original dielectric strength for a longer time.

Following this section, Experimental section describes the experimental details, including the raw materials, sample preparation, aging condition, and characterization methods. The results of the dielectric measurements are presented and discussed in Results and Discussion section. Finally, conclusions are drawn in Conclusions section.

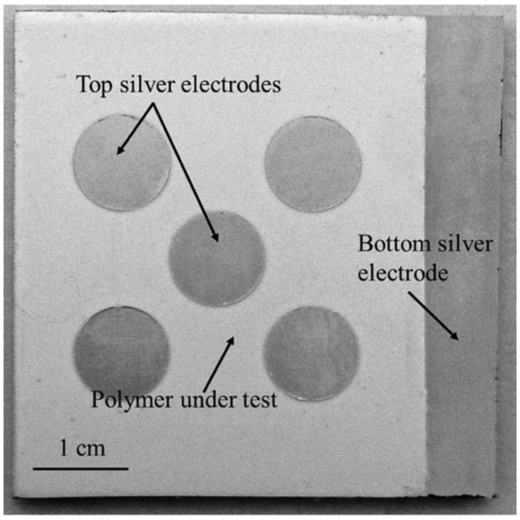

Figure 1. Top view of tester for dielectric characterization.

EXPERIMENTAL

Fabrication of Al_2O_3/Silicone Composites

Silicone elastomer (EPM-2422, Nusil Technology) and Al_2O_3 fiber (Part No. 43912, Alfa Aesar) were used as the polymer matrix and the filler, respectively. Mesitylene (C_9H_{12}) was used as a solvent to dilute the viscous silicone for better filler dispersion. Silicone (EPM-2422 part A), Al_2O_3 fibers (0, 10, 15, or 30 wt %), and mesitylene (approximately the same volume as the silicone in use) were mixed by ultrasonic agitation (ViSonic 475 ultrasonic agitator) in an ice-water bath. The detailed procedure for ultrasonic agitation was reported earlier in Ref. 21. The resulting mixture was heated up to 175°C by a hot plate in a vented hood to remove mesitylene. A stir bar was used to speed up the evaporation process, which took about 4 h. The mixture of EPM-2422 part A and Al_2O_3 fibers was then cooled down to room temperature before part B was added into it according to the mixing ratio specified by the manufacturer (part A : part B = 10 : 1 by weight). The as-prepared mixture was then immediately used to prepare the tester for dielectric-strength measurements.

Preparation of Tester for Dielectric Characterization

A tester with a flat polymer film (material under test) sandwiched between two electrodes was designed. A flat glass substrate (5 cm × 5 cm) was sputter-coated with a Cr/Ni/Ag tri-layer by physical vapor deposition. Uncured Al_2O_3/silicone composite (immediately used after preparation to prevent viscosity increase) was spin-coated on top of the metallized glass substrate, with the thickness controlled to approximately 100 μm. The composite was then cured in air at 65°C for 4 h. Five silver electrodes were painted on the cured composite film by using a silver paste (NanoTach X, NBE Technology). The tester was then placed on a hot plate at 250°C for 10 min to sinter the silver electrodes. Figure 1 shows the top view of the tester for dielectric characterization.

Characterization of Dielectric Strength

The dielectric strength of the composite film was measured by Hipot Megohmmeter 200B, whose cathode and anode were connected to the top and bottom electrodes of the dielectric tester, respectively. The test was performed with AC voltage, which was ramped up at a constant rate until breakdown was detected by Hipot. The maximum voltage prior to breakdown was recorded as the breakdown voltage, V_{BD}. The thickness of the film, t, was measured by a micrometer. The dielectric strength, E_{BD}, was calculated by dividing the breakdown voltage by the thickness of the sample, as expressed by the following equation:

$$E_{BD} = \frac{V_{BD}}{t} \qquad (1)$$

Thermal Aging

To investigate the effect of Al_2O_3 fibers on thermal stability of silicone, we prepared dielectric testers (Figure 1) made of unfilled silicone and Al_2O_3/silicone composites with fiber loading of 10, 15, and 30 wt % for thermal aging in an environmental chamber (Model 9023, Delta Design) at 250°C—the maximum operation temperature of current SiC devices. At the beginning of aging, the temperature was ramped up from room temperature to 250°C in 20 min and maintained there throughout the test. During aging, the temperature variation was kept within ±0.5°C. At least two testers were removed from the furnace at each sampling point and their dielectric strength was soon measured after the tester was cooled down to room temperature. The sampling points used in this study were 80, 160, 240, 320, 400, and 480 h.

Scanning Electron Microscopy

To explain the relationship between the silicone degradation and the low dielectric strength, we examined the aged testers made of unfilled and silicone filled with 15 wt % of Al_2O_3 by scanning electron microscopy (SEM) after dielectric measurements. The experiment was performed with a LEO (Zeiss) 1550 field-emission SEM. An accelerating voltage of 5 kV was used to avoid overheating or degrading the polymer film. In-lens detector that mainly collects backscattered electrons was used. The top surface of dielectric tester was gently cleaned with ethanol and sputter-coated with gold (a few nanometers in thickness) before SEM observation. During the experiment, the top electrodes and the polymer film adjacent to them were carefully examined to find signs of defect development that are responsible for dielectric failure.

RESULTS AND DISCUSSION

Dielectric Strength of As-Prepared Al_2O_3/Silicone Composites

The test results of dielectric breakdown of polymers are often analyzed with a statistical method. The Weibull distribution is widely accepted for such data analysis because dielectric failure of an entire system depends on that of the weakest point.[22,23] The probability of failure, P, at a given electric field follows the mathematical expression of

$$P = 1 - \exp\left[-\left(\frac{E}{E_0}\right)^{\beta}\right] \qquad (2)$$

where E is the applied field and E_0 and β are the Weibull parameters. E_0 is the characteristic dielectric strength that represents the electric field at which the failure probability is 63.2%. β is the shape parameter that measures the spread of the data.

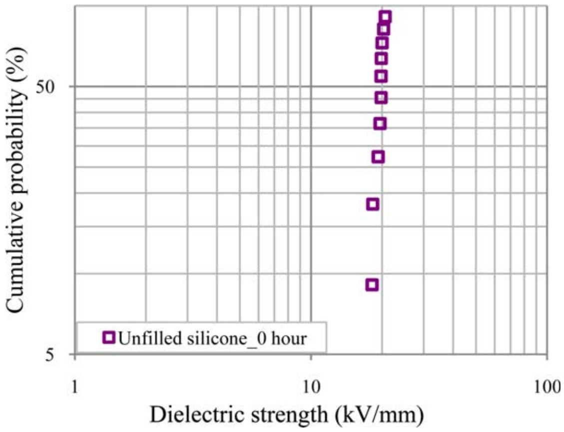

Figure 2. Weibull plot of measured dielectric strength of as-prepared unfilled silicone. [Color figure can be viewed in the online issue, which is available at wileyonlinelibrary.com.]

The higher the β, the narrower the distribution. The calculation of the two parameters as well as their confidence interval of 90% was based on the methods given in Refs. 24,25.

The Weibull plot of the breakdown data from as-prepared unfilled silicone (which was prepared according to the procedure described in Fabrication of Al_2O_3/Silicone Composites except that no Al_2O_3 fiber was added) is shown in Figure 2. The characteristic dielectric strength and shape parameter of this sample are listed in Table I. E_0 of the unfilled silicone ($\sim$20 kV/mm) falls in the typical range of dielectric strength of silicone.[5,6] The narrow distribution observed on the Weibull plot yielded a β of $>$15. The Weibull plots of the breakdown data from as-prepared Al_2O_3/silicone composites with fiber loadings of 10, 15, and 30 wt % are shown in Figure 3. The two Weibull parameters for these samples are also listed in Table I. The characteristic dielectric strength of all three composites is comparable to that of the unfilled silicone. The data obtained from the three composites also show a narrow distribution on the Weibull plot, with $\beta > 15$. Such results clearly indicate that the Al_2O_3 fibers had no adverse impact on the insulation capability of the silicone encapsulant.

Effect of Thermal Aging on Dielectric Strength of Unfilled Silicone

Dielectric testers built with unfilled silicone were aged isothermally at 250°C in air for at least 480 h. Within 200 h of aging, the silicone film showed no change in physical appearance under optical microscope. The Weibull plots of unfilled silicone aged for up to 480 h are shown in Figures 4 and 5. The dielectric data for the unfilled silicone aged for 80 h exhibit good consistency, with a large β-value of 23.14. E_0 of the unfilled silicone aged for 80 h was calculated to be 20.82 kV/mm, which was comparable to that of the as-prepared one. As aging continued to 160 and 200 h, dielectric failure below 15 kV/mm was detected. Such early failure could be explained by the formation of microscale cracks and voids as a result of silicone degradation. Both cracks and voids are considered as cavities in the matrix and are filled with air, which has much lower dielectric strength than the polymer matrix. When a cavity is large enough, it is possible that during measurement the electric field in the cavity reaches the dielectric strength of air before breakdown occurs in the polymer matrix. Partial discharge could then occur in the cavity and damage the polymer matrix, leading to electrical breakdown of the entire film.

As aging continued to 240 h, dielectric failure below 15 kV/mm occurred more frequently. In the meantime, a few visible macroscale cracks appeared in the polymer matrix. A similar phenomenon was observed in dielectric testers aged for 320 h as well. The cracks identified in such samples were found to propagate through the entire thickness of the polymer film. If the crack happens to be very close to (e.g., <0.5 mm from) a top

Table I. Characteristic Dielectric Strength and Shape Parameter of As-Prepared Unfilled and AL_2O_3-Filled Silicones

As-prepared (Unaged)[a]	0 wt %	10 wt %	15 wt %	30 wt %
E_0 (kV/mm)	20.13	22.30	20.27	20.67
β	33.82	41.26	22.55	41.60

[a] No crack observed in any of the samples.

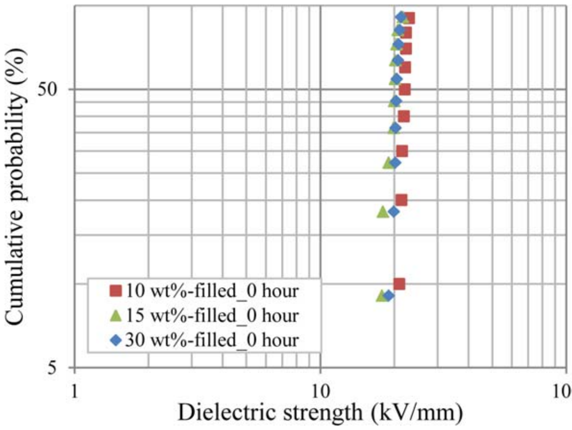

Figure 3. Weibull plots of measured dielectric strength of as-prepared Al_2O_3/silicone composites. [Color figure can be viewed in the online issue, which is available at wileyonlinelibrary.com.]

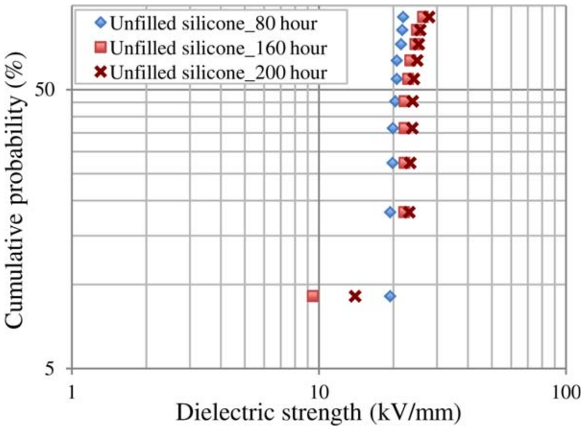

Figure 4. Weibull plots of measured dielectric strength of unfilled silicone aged for 80, 160, and 200 h. [Color figure can be viewed in the online issue, which is available at wileyonlinelibrary.com.]

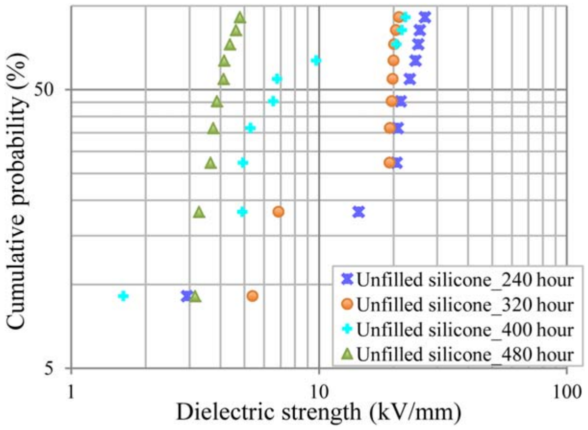

Figure 5. Weibull plots of measured dielectric strength of unfilled silicone aged for 240, 320, 400, and 480 h. [Color figure can be viewed in the online issue, which is available at wileyonlinelibrary.com.]

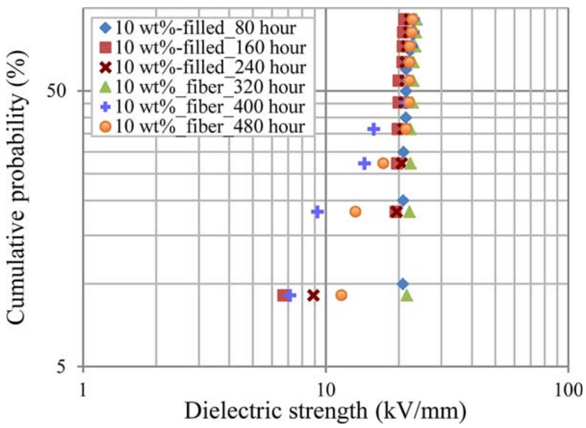

Figure 7. Weibull plots of measured dielectric strength 10-wt %-filled silicone aged for up to 480 h. [Color figure can be viewed in the online issue, which is available at wileyonlinelibrary.com.]

electrode, the dielectric strength obtained from that electrode may be impaired owing to the reduction of creepage distance. The dielectric failure below 15 kV/mm observed in samples aged for 240 and 320 h could be explained this way. The area where a top electrode was not impacted by cracks maintained a high dielectric strength of approximately 20 kV/mm, which was comparable to the result obtained from the as-prepared silicone. As only a small fraction of data points (∼20%) was impacted by cracks in the silicone film, the characteristic dielectric strength was still higher than 20 kV/mm. However, cracks adjacent to top electrodes caused a wide distribution of data points and thus significantly reduced the shape parameter as shown in Figure 6.

As aging continued to 400 h, cracks were more frequently found in the silicone film and started to form a network, resulting in a significant decrease of dielectric strength in most of the measurements as shown in Figure 5. As 70% of the data exhibit dielectric strength below 10 kV/mm, the characteristic dielectric strength, which represents the value corresponding to a failure probability of 63.2%, is reduced dramatically to 10.60 kV/mm. In the meantime, as a few measurements are still not severely impacted by cracks around top electrodes, a wide distribution of data points is observed, resulting a very small β of 1.18. After 480 h of aging, all top electrodes were severely impacted by cracks, resulting in a dielectric strength lower than 5 kV/mm in each measurement as shown in the Weibull plot (Figure 5). The characteristic dielectric strength is further reduced to 4.11 kV/mm. The shape parameter, however, is restored to 7.73 owing to the consistency in failure mechanism.

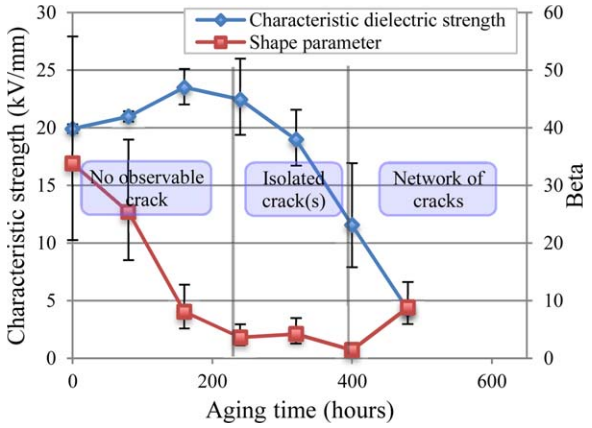

Figure 6. Variation in Weibull parameters of unfilled silicone with time of thermal aging. [Color figure can be viewed in the online issue, which is available at wileyonlinelibrary.com.]

The variations of the two Weibull parameters of unfilled silicone with aging time are plotted in Figure 6. The E_0 remains above 20 kV/mm for 240 h when the integrity of most of the silicone film remained intact, but dramatically decreases after 320 h when a large fraction (≥63.2%) of the data points were impacted by cracks. When all data points fall below 5 kV/mm after 480 h of aging, E_0 reaches the minimum of 4.11 kV/mm, which is comparable to the dielectric strength of air at that thickness. In contrast, β is more sensitive to the degradation of the silicone film. Even before cracks could be observed by optical microscope (after 160 h of aging), β reduces to below 5 by the occasional dielectric failure below 15 kV/mm. β-Value remains low (<5) until all measurements are impacted by cracking and all data points fall below 5 kV/mm after 480 h.

Effect of Thermal Aging on Dielectric Strength of Al_2O_3/Silicone Composites

Al_2O_3/silicone composites with fiber loading of 10, 15, and 30 wt % were also used to fabricate dielectric testers, which were then subjected to thermal aging at 250°C before dielectric measurements. None of the dielectric testers made of a composite exhibited noticeable change in physical appearance under optical microscope throughout the entire aging period. The Weibull plots of the measured dielectric strength of composite filled with 10 wt % of Al_2O_3 fibers are shown in Figure 7. For this composite, as for the unfilled silicone, dielectric failure below 15 kV/mm begins after 160 h of aging, causing reduction of shape parameter. The dielectric strength measured on composite filled with 10 wt % of Al_2O_3 fibers after 320 h of aging is found to be an exception: no dielectric failure below 15 kV/mm is detected in the test, causing a large β-value. The occurrence of dielectric failure relies on the existence and the development of

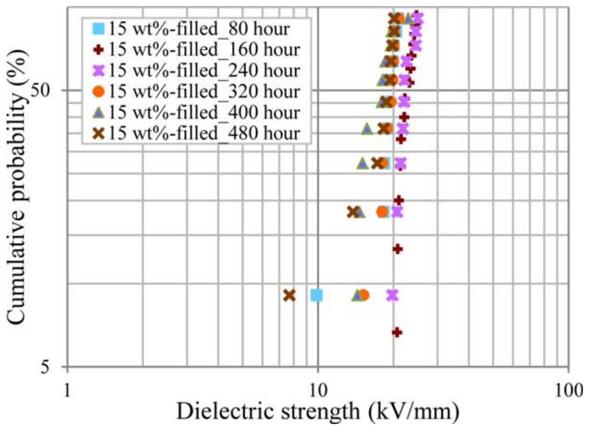

Figure 8. Weibull plots of measured dielectric strength of 15-wt %-filled silicone aged for up to 480 h. [Color figure can be viewed in the online issue, which is available at wileyonlinelibrary.com.]

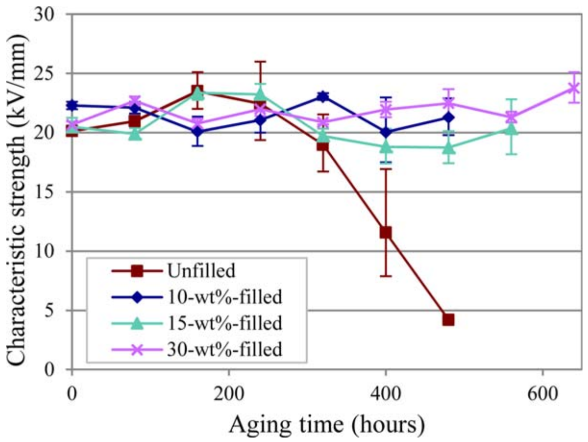

Figure 10. Variation in characteristic dielectric strength of unfilled and Al_2O_3-filled silicones with aging time. [Color figure can be viewed in the online issue, which is available at wileyonlinelibrary.com.]

defects, which is random and is rare at the beginning stage of degradation. Therefore, a much larger sample population may help to reduce the error in β calculation.

The Weibull plots of dielectric strength measured on the 15-wt %-filled composite are shown in Figure 8. For up to 320 h of aging, dielectric failure rarely occurs below 15 kV/mm, with only one exception observed at 80 h. Such unusual behavior (failure at $\sim$10 kV/mm) of the composite film ages for 80 h could be explained by occasional manufacture defects created during sample preparation (e.g., spin-coating, curing, etc.). After 320 h of aging, the data points start to exhibit a slightly wider spread of data points on the Weibull plot, possibly indicating that the integrity of polymer film has been impaired. After longer aging time, dielectric failure is more likely to occur below the typical value of 20 kV/mm, resulting in an even wider spread of data points on Weibull plot and a smaller shape parameter.

The Weibull plots of dielectric strength measured on the 30-wt %-filled composite are shown in Figure 9. For up to 400 h of aging, dielectric failure rarely occurs below 15 kV/mm, with only one exception observed at 160 h. This unusual behavior could also be explained by the defects introduced into the composite during sample preparation. At 320 h, a large β-value with a wide confidence interval is observed and is again owing to the randomness of defect existence and development. After 480 and 560 h of aging, dielectric failure below 15 kV/mm is detected because of the degradation of film integrity, widening the distribution of data points, and reducing the β-value.

Figures 10 and 11 show the plots of characteristic dielectric strength and shape parameter, respectively, against aging time for unfilled and filled silicones. E_0 of the unfilled silicone exhibits a dramatic decrease after 320 h, which is caused by the formation of a network of macroscale cracks developed in the silicone film during aging. E_0 of the Al_2O_3/silicone composites with fiber loading of 10, 15, and 30 wt % remains at approximately 20 kV/mm throughout the entire aging period. However, the variation of each data point, as expressed by the error bars, becomes larger after longer aging time, indicating that the integrity of the composite films has been gradually impaired. These results suggest that Al_2O_3 fibers could effectively improve the

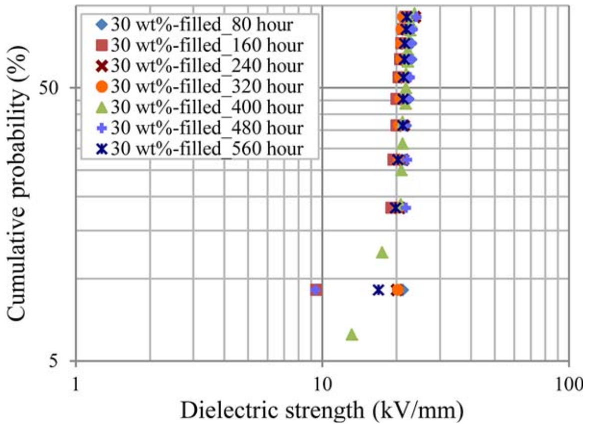

Figure 9. Weibull plots of measured dielectric strength of 30-wt %-filled silicone aged for up to 560 h. [Color figure can be viewed in the online issue, which is available at wileyonlinelibrary.com.]

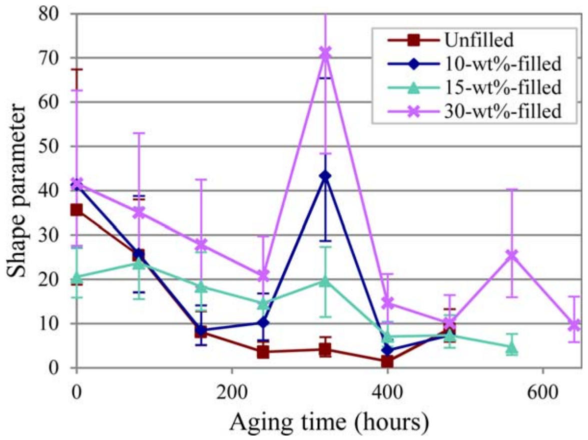

Figure 11. Variation in shape parameter of unfilled and Al_2O_3-filled silicones with aging time. [Color figure can be viewed in the online issue, which is available at wileyonlinelibrary.com.]

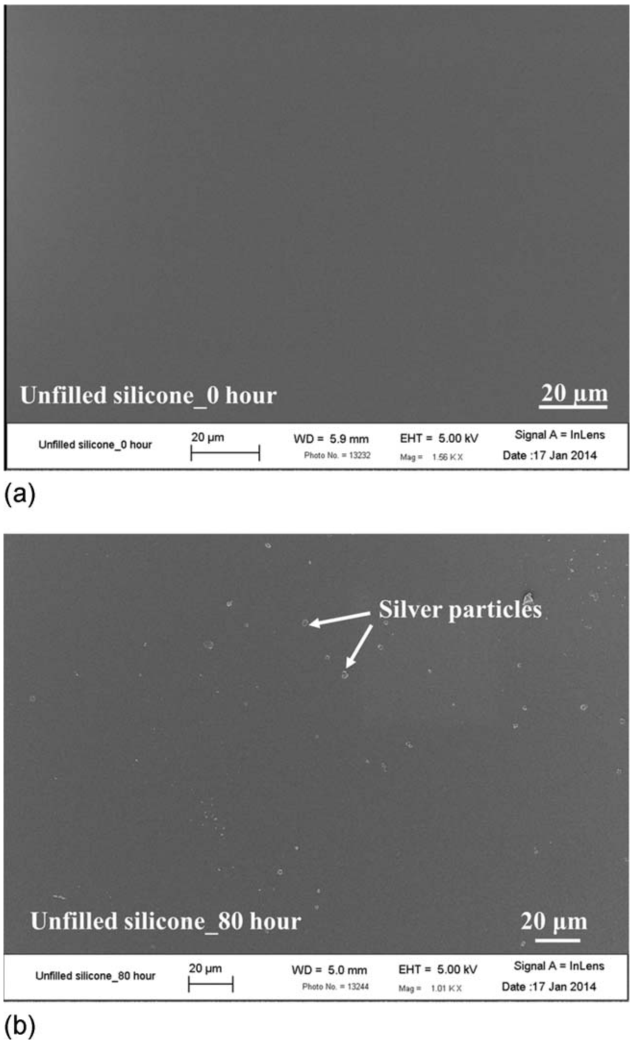

Figure 12. SEM images of unfilled silicone: (a) before aging and (b) aged for 80 h.

thermal stability of silicone. The same conclusion can also be drawn by considering the change of shape parameter with aging time. The β of unfilled and 10-wt %-filled silicone exhibits a dramatic decrease after 160 h owing to the development of cracks and defects caused by quick degradation during thermal aging. The β-value of the Al_2O_3/silicone composite with a fiber loading of 15 wt % exhibits a gradual decrease with aging time and remains above 5 for 400 h, indicating an improved thermal stability over that of the unfilled and 10-wt %-filled silicones. The β of the Al_2O_3/silicone composite with a fiber loading of 30 wt % remains the highest of all materials studied. The increase in β with increasing fiber loading also indicates that the thermal stability of silicone is improved by the addition of Al_2O_3 fibers and that the 30-wt %-filled composite has the highest thermal stability.

Effect of Thermal Aging on Silicone Degradation

The polymer film in the dielectric tester was subjected to elastic stresses caused by the mismatch of coefficients of thermal expansion (CTE) of the polymer film and the glass substrate when the tester was cooled down to room temperature after the long-term annealing in furnace at 250°C. The stress increases with increasing elastic/storage modulus of the polymer. When exposed to high temperature, for example, 250°C, silicone suffers from severe degradation, involving scission of the polysiloxane chain and generation of volatile species.[26–28] Shortening of the chain leads to an increase in crosslink density and therefore a higher storage modulus, which then results in higher stresses caused by the CTE mismatch.

Flexibility of silicone is also impaired by the degradation process in which the long polysiloxane chains were shortened, embrittling the polymer matrix. Therefore, as aging continued, the silicone film in the dielectric tester suffered from both higher elastic stress and matrix embrittlement. When the film was no longer strong enough to maintain its integrity, cracking would occur. Any void that was produced during either manufacture or degradation could assist in crack initiation and propagation. As a result, thermal aging at 250°C was expected to introduce defects in the silicone matrix and damage the film integrity, causing dielectric failure to occur at a lower electric field. The development of defects in the aged silicone matrix was examined by SEM, with the results shown in the next section.

Scanning Electron Microscopy

Dielectric testers made with unfilled and Al_2O_3-filled silicones were examined by SEM after dielectric measurements. The results were expected to help explain the effect of thermal aging on the degradation of silicone matrix and dielectric strength observed even before macroscale cracks appeared in the aged film. The SEM image of the as-prepared unfilled silicone, serving as the benchmark for comparison, is shown in Figure 12(a). The as-prepared silicone exhibits a flat surface in the absence of noticeable defects (e.g., cracks and voids). After 80 h, no change in physical appearance can be seen as shown in Figure 12(b). The silicone film maintains its integrity and shows no noticeable defect, explaining the high dielectric strength (~20 kV/mm) of the film aged for 80 h. A few particles (also seen on the surface of as-prepared silicone) are found on the silicone film and are believed to be debris from top silver electrodes during the cleaning process prior to SEM examination.

As aging continues, microscale cracks gradually appear in polymer matrix, as indicated by the arrow in Figure 13. Such cracks are too small to be seen under optical microscope; however, they can still have a significant impact on the insulation capability of the silicone film. When a microcrack appears adjacent to a top electrode, dielectric failure measured from that electrode could occur at a lower electric field owing to the reduction of creepage distance or partial discharge in the cracked region.

The SEM image of the unfilled silicone aged for 320 h are shown in Figure 14. Macroscale cracks measuring a few tens of micrometers in width are also visible under optical microscope. Such cracks usually stop propagating when approaching a top electrode, where the stress caused by CTE mismatch can be slightly released by the ductile silver film (electrode). SEM also confirms that microscale cracks tend to initiate from a large one, forming a network of cracks in silicone films aged for even

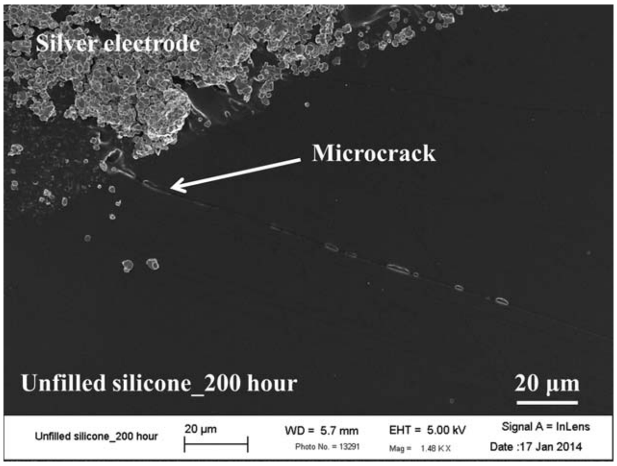

Figure 13. SEM image of unfilled silicone aged for 200 h.

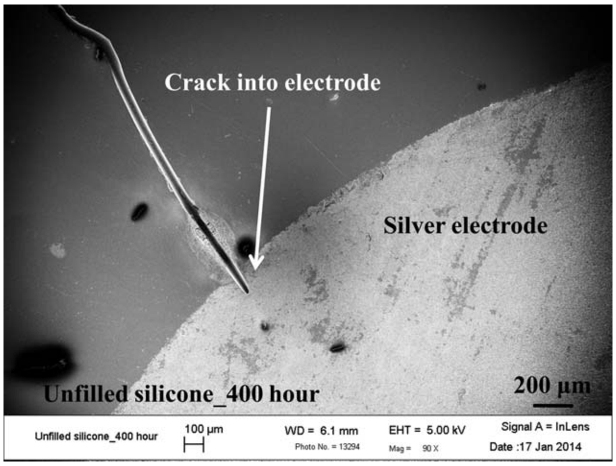

Figure 15. SEM image of unfilled silicone aged for 400 h.

longer times. The SEM images of the unfilled silicone aged for 400 h are shown in Figure 15. After 400 h, cracks propagate directly into a top electrode, indicating that the polymer has become more brittle with further aging. The SEM images clearly demonstrate that the degradation of silicone causes the development of cracks in the matrix, which is responsible for dielectric failure at low electric field.

The microstructure evolution in the aged Al_2O_3/silicone composite with a 15 wt % fiber loading was also examined by SEM. After 80 h of aging, the composite film exhibits no defect as shown in Figure 16. However, the surface of the composite, with wrinkle-like structures around agglomerates of Al_2O_3 fibers measuring 2–5 µm, is obviously rougher than that of the unfilled silicone [Figure 12(b)] at the same aging time. The wrinkle-like structure is observed on all composite surfaces and is probably formed during the curing process when the silicone tends to slightly shrink, whereas the chain movement is anchored by the surface of large agglomerates, causing nonuniform shrinkage of the composite film.

After 240 h of aging, the composite film still maintains its integrity [Figure 17(a)], explaining the absence of dielectric failure below 20 kV/mm (Figure 8). The slower degradation of the composite than that of the unfilled silicone is attributed to the filler–matrix interaction, which restrained chain mobility and decelerated the chain-scission process as confirmed in our previous study.[21] However, possible initiation of microscale cracks is observed in the composite with a fiber loading of 15 wt % after 240 h of aging as shown in Figure 17(b). The initiation site is near the Al_2O_3/silicone interface, where the stress condition may be different from that in the matrix far from the interface. The microscale crack observed at this stage has no significant effect on dielectric strength as demonstrated by the test results explained in Effect of Thermal Aging on Dielectric Strength of Al_2O_3/Silicone Composites section. Although the sign of crack initiation indicates an ongoing degradation of the polymer matrix, such initiation occurs after a much longer aging time in the composite than in the unfilled silicone, an indication that the thermal stability is enhanced by Al_2O_3 fibers.

After 480 h of aging, microcracks similar to those observed in the unfilled silicone aged for 200 h are observed as shown in Figure 18. The corresponding dielectric results presented in Effect of Thermal Aging on Dielectric Strength of Al_2O_3/Silicone Composites section showed that dielectric failure could occur at an electric field much lower than 20 kV/mm. Therefore, in both

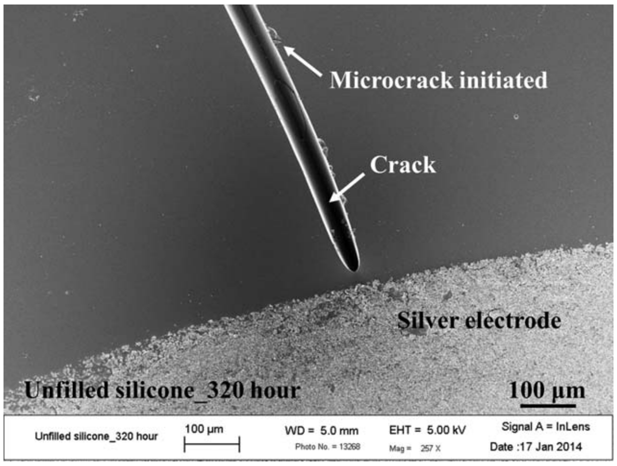

Figure 14. SEM image of unfilled silicone aged for 320 h.

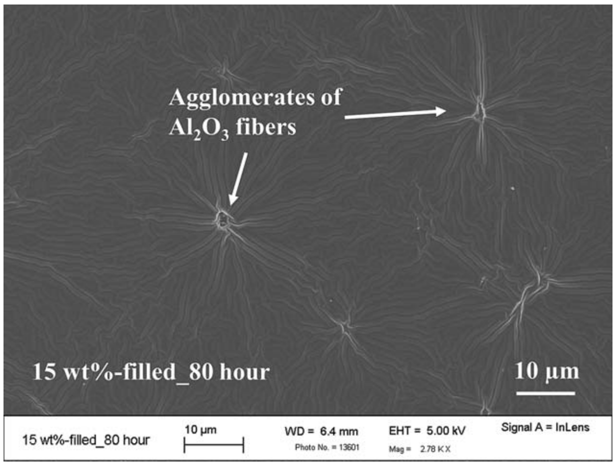

Figure 16. SEM image of Al_2O_3/silicone composite with a fiber loading of 15 wt % after 80 h of aging.

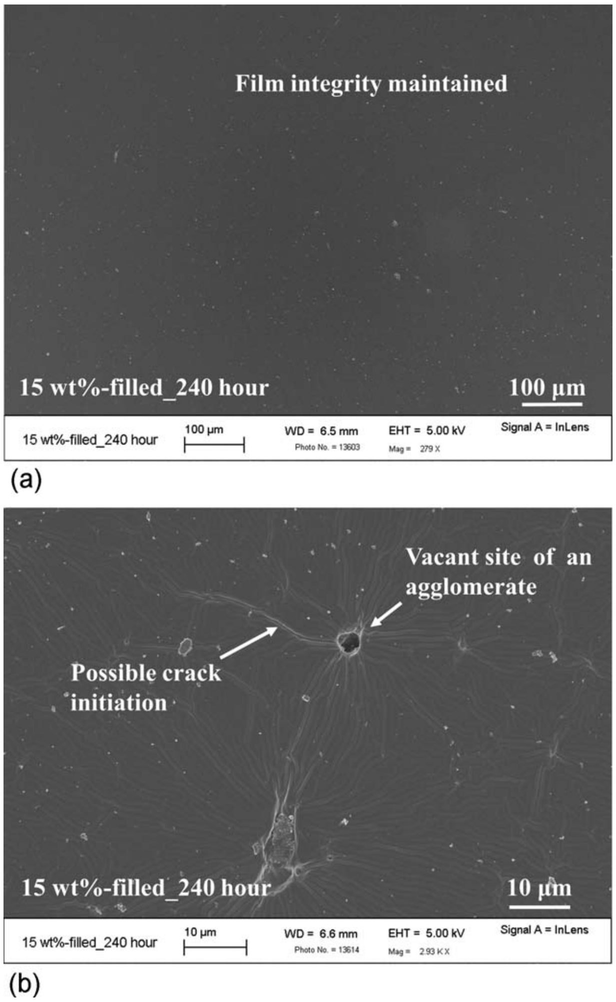

Figure 17. SEM images of Al_2O_3/silicone composite with a fiber loading of 15 wt % after 240 h of aging: (a) integrity of composite film maintained and (b) crack initiation around Al_2O_3 fillers.

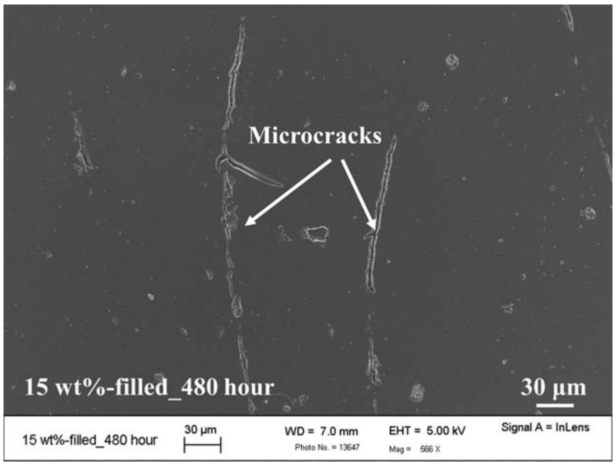

Figure 18. SEM image of Al_2O_3/silicone composite with a fiber loading of 15 wt % after 480 h of aging.

unfilled and filled silicones, even microcracks that are not visible to the eyes and under optical microscope could significantly affect the dielectric behavior. The microcracks are a result of silicone degradation caused by long-term thermal aging, which shortens the flexible polysiloxane chains and embrittles the matrix. It obviously takes longer time for the defects to develop in the composite, which was shown in our previous study[21] to exhibit slower degradation and higher thermal stability than the unfilled silicone. As a result, the degradation of dielectric strength, as represented by the decrease of both characteristic dielectric strength and shape parameter from Weibull plots, with aging time, was also observed to be slower in the composite than in the unfilled silicone.

CONCLUSIONS

To investigate the effect of Al_2O_3 fibers on the thermal stability of silicone, the dielectric strength of silicone filled with various loading of Al_2O_3 fibers, including 0, 10, 15, and 30 wt %, was compared before and after thermal aging at 250°C in air. The results of the dielectric measurements were analyzed by using Weibull distribution. The two Weibull parameters obtained in the statistical analysis were used to compare the dielectric behavior of unfilled silicone and the composites. The dielectric strength prior to thermal aging was first compared. The characteristic dielectric strength (E_0) of the unfilled silicone was measured to be 20.13 kV/mm, whereas that of the Al_2O_3/silicone composites with fiber loading of 10, 15, and 30 wt % were 22.30, 20.27, and 20.67 kV/mm, respectively. The measured shape parameter (β) was above 15 for the four materials. This narrow distribution on the Weibull plot indicated the consistency of dielectric failure observed in all samples prior to aging. Such results clearly demonstrated that the Al_2O_3 fibers added into the silicone matrix had no detrimental effect on the dielectric strength.

The thermal stability of the unfilled silicone and its composites was represented by the degradation in their dielectric performance with respect to the time of thermal aging performed at 250°C in air. For unfilled silicone, microcracks were seen by SEM after 200 h of aging and macrocracks appeared after 320 h. In contrast, microcracks that comparable to those observed in unfilled silicone after 200 h appeared in the Al_2O_3/silicone composite after a much longer time (480 h). No macrocrack was found in the composite throughout the entire aging period. E_0 of the unfilled silicone decreased dramatically after 320 h of aging, meaning that most of the measurements were impacted by macro- or microscale cracks developed in the silicone film as a result of thermal degradation. E_0 of the Al_2O_3/silicone composites showed no significant change throughout the entire 560 h of aging. β was more sensitive to silicone degradation because even a small portion of the dielectric failure detected at low electric fields owing to the presence of cracks could cause a wide distribution. β of the unfilled silicone decreased significantly to approximately one after 160 h of aging, whereas that of the Al_2O_3/silicone composite with 15 wt % fiber loading decreased gradually to a similar value after 480 h and that of the composite with 30 wt % of fiber loading remained the highest among the values of the four materials throughout the entire aging time. The change of both Weibull parameters with aging time indicated that unfilled silicone had the lowest thermal stability, which increased monotonically with increasing loading of Al_2O_3 fibers.

ACKNOWLEDGMENTS

This study was supported by the High Density Integration (HDI) mini-consortium of the Center for Power Electronics Systems (CPES) at Virginia Tech. The authors are grateful to helpful comments from Dr. Wenli Zhang and Dr. Kewei Xiao of CPES.

REFERENCES

1. Wong, C. P. *IEEE Trans. Comp. Packag. Manuf. Technol. A* **1995**, *18*, 270.
2. Wong, C. P. *Adv. Polym. Sci.* **1988**, *84*, 63.
3. Yao, Y.; Seshadri, J.; Lu, G.; Ngo, K. D. T. Assessment of high-temperature encapsulants for planar package, Proceedings of the SAE Power Systems Conference, Fort Worth, TX, November 2–4, 2010, DOI:10.4271/2010-01-1729.
4. EPM-2482-Technical Data Sheet. Available from: http://nusil.com/products/ProductProfiles/EPM-2482/EPM-2482P.pdf.
5. 500°F-800°F Duraseal$^+$ Silicones. Available from: http://www.cotronics.com/vo/cotr/pdf/1531.pdf.
6. R-2188-Technical Data Sheet. Available from: http://nusil.com/products/ProductProfiles/R-2188/R-2188P.pdf.
7. Scofield, J. D.; Merrett, J. N.; Richmond, J.; Agarwal, A.; Leslie, S. Performance and reliability characteristics of 1200 V, 100 A, 200°C half-bridge SiC MOSFET-JBS diode power modules. Proceedings of the International Conference on High Temperature Electronics (HiTEC), Albuquerque, NM, May 11–13, **2010**.
8. Yao, Y.; Chen, Z.; Lu, G.; Boroyevich, D.; Ngo, K. D. T. *IEEE Trans. Comp. Packag. Manuf. Technol.* **2012**, *2*, 539.
9. Sohoni, G. B.; Mark, J. E. *J. Appl. Polym. Sci.* **1992**, *45*, 1763.
10. El-Hag, A. H.; Simon, L. C.; Jayaram, S. H.; Cherney, E. A. *IEEE Trans. Dielectr. Electr. Insul.* **2006**, *13*, 122.
11. Yang, L.; Qiu, S.; Zhang, Y.; Xu, Y. *J. Polym. Res.* **2013**, *20*, 1.
12. Sim, L. C.; Ramanan, S. R.; Seetharamu, H. N.; Goh, T. J. *Thermochim. Acta* **2005**, *430*, 155.
13. Xiong, Y.; Shen, Q.; Chen, F.; Luo, G.; Yu, K.; Zhang, L. *Fire Mater.* **2012**, *36*, 254.
14. Amendola, E.; Lupo, G.; Petrarca, C.; Scamardella, A. M. *Int. J. Appl. Electrom.* **2012**, *39*, 3.
15. Zhou, W.; Qi, S.; Tu, C.; Zhao, H. *J. Appl. Polym. Sci.* **2007**, *104*, 2478.
16. Garg, P.; Singh, R. P.; Choudhary, V. *Sep. Purif. Method* **2011**, *80*, 435.
17. Kong, Q.; Hu, Y.; Song, L.; Wang, Y.; Chen, Z.; Fan, W. *Polym. Adv. Technol.* **2006**, *17*, 463.
18. Yang, L.; Hu, Y.; Lu, H.; Song, L. *J. Appl. Polym. Sci.* **2006**, *99*, 3275.
19. Kim, J. W.; Noh, M. H.; Choi, H. J.; Lee, D. C.; Jhon, M. S. *Polymer* **2000**, *41*, 1228.
20. Zhou, W.; Qi, S.; Zhao, H.; Liu, N. *Polym. Compos.* **2007**, *28*, 23.
21. Yao, Y.; Lu, G.; Boroyevich, D.; Ngo, K. D. T. *Polymer* **2014**, DOI: 10.1016/j.polymer.2014.05.044.
22. Chen, G.; Davis, A. V. *IEEE Trans. Dielectr. Electr. Insul.* **2000**, *7*, 401.
23. Coppard, R. W.; Bowman, J.; Dissado, L. A.; Rowland, S. M.; Rakowski, R. T. *J. Phys. D Appl. Phys.* **2000**, *23*, 1554.
24. IEEE Std 930$^{\text{TM}}$−2004. IEEE Guide for the Statistical Analysis of Electrical Insulation Breakdown Data. April **2005**.
25. Stone, G. C.; van Heeswijk, R. G. *IEEE Trans. Electr. Insul.* **1977**, *EI-0000*, 253.
26. Grassie, N.; MacFarlane, I. G. *Eur. Polym. J.* **1978**, *14*, 875.
27. Camino, G.; Lomakin, S. M.; Lageard, M. *Polymer* **2002**, *43*, 2011.
28. Camino, G.; Lomakin, S. M.; Lageard, M. *Polymer* **2001**, *42*, 2395.